

10-8-1996

# Electronic Spectroscopy of Jet-Cooled Benzylidenecyclobutane, a Sterically Hindered Styrene

John R. Cable

*Bowling Green State University - Main Campus*, [cable@bgsu.edu](mailto:cable@bgsu.edu)

V.P. Manea

Follow this and additional works at: [http://scholarworks.bgsu.edu/chem\\_pub](http://scholarworks.bgsu.edu/chem_pub)

 Part of the [Chemistry Commons](#)

---

## Repository Citation

Cable, John R. and Manea, V. P., "Electronic Spectroscopy of Jet-Cooled Benzylidenecyclobutane, a Sterically Hindered Styrene" (1996). *Chemistry Faculty Publications*. Paper 30.  
[http://scholarworks.bgsu.edu/chem\\_pub/30](http://scholarworks.bgsu.edu/chem_pub/30)

This Article is brought to you for free and open access by the Chemistry at ScholarWorks@BGSU. It has been accepted for inclusion in Chemistry Faculty Publications by an authorized administrator of ScholarWorks@BGSU.

# Electronic spectroscopy of jet-cooled benzylidenecyclobutane, a sterically hindered styrene

V. P. Manea and J. R. Cable

Department of Chemistry and Center for Photochemical Sciences, Bowling Green State University, Bowling Green, Ohio 43403

(Received 13 May 1996; accepted 25 June 1996)

The electronic spectrum of the styrene derivative, benzylidenecyclobutane, seeded in a supersonic jet expansion has been recorded using resonantly enhanced two-photon ionization spectroscopy. The main vibronic features in the spectrum are associated with a low frequency progression assigned to the torsional motion of the phenyl ring. Analysis of the observed torsional levels reveals an excited state potential energy surface characteristic of a planar equilibrium geometry which undergoes large amplitude motion and a ground state surface having a minimum at a torsional angle of  $25^\circ$  between the phenyl and vinyl groups. *Ab initio* calculations of the ground state torsional potential surface predict a minimum in the range of  $28^\circ$ – $26^\circ$ , depending on the size of the basis set. In these structures the cyclobutane ring adopts a puckering angle between  $17^\circ$  and  $19^\circ$ . Deuterated isotopomers have also been synthesized and their corresponding photoionization spectra analyzed to reveal the mixing between the torsion and other low frequency modes such as cyclobutane ring puckering. The extent of this mixing is found to be sensitive to the sites of deuteration on the molecule. © 1996 American Institute of Physics. [S0021-9606(96)00337-6]

## I. INTRODUCTION

A variety of spectroscopic techniques have been used to explore the phenyl torsional motion in styrene and its substituted derivatives<sup>1–10</sup> and its relation to the *cis*–*trans* double bond isomerization process.<sup>11–13</sup> The planarity of styrene in the  $S_0$  and  $S_1$  electronic states has been determined from analysis of both the  $S_1 \rightarrow S_0$  laser induced single vibronic level fluorescence spectra as well as the corresponding excitation spectra.<sup>3,4</sup> Planarity of the ground state has also been confirmed by microwave spectroscopy.<sup>5</sup> In  $S_0$  torsion occurs on a very shallow flat-bottomed potential having an estimated barrier of  $1070 \text{ cm}^{-1}$  at the perpendicular geometry.<sup>4</sup> The torsional potential energy surface reflects the dominance of the stabilizing effects of conjugation over the destabilization induced by steric repulsive interactions which are also maximized at the planar conformation.

When the magnitudes of the steric forces are increased, deviations from a planar structure will occur as when  $\alpha$  or *cis*- $\beta$  substituents are added to the vinyl group. For instance,  $\alpha$ -methyl-styrene has been determined to be nonplanar in  $S_0$ , with a torsional angle of  $30^\circ$ , but planar in  $S_1$ .<sup>8</sup> In this case, electronic factors dictate the  $S_1$  geometry while steric destabilization is more important in  $S_0$ . Similarly in the  $\alpha$ -substituted derivative 1-phenylcyclohexene, electronic spectroscopy from this laboratory has been used to identify two inequivalent ground state conformers with phenyl torsional angles of  $\pm 27^\circ$ , which differed in energy by  $127 \text{ cm}^{-1}$ .<sup>14</sup> The excited state of this molecule was also determined to have a torsional angle of  $0^\circ$ .

Spectroscopic investigations of these sterically hindered styrenes were extended in a recent study to derivatives substituted at the  $\beta$  position of the ethylenic bond.<sup>15</sup> Two  $\beta$ -cycloalkane derivatives, benzylidenecyclopentane and benzylidenecyclohexane, were synthesized and their reso-

nantly enhanced two-photon ionization spectra analyzed. Both compounds were found to undergo large changes in torsional geometry following photoexcitation leading to estimates of the ground state torsional angle of approximately  $45^\circ$  in benzylidenecyclopentane<sup>16</sup> and  $50^\circ$  in benzylidenecyclohexane. The greater deviation from planarity in benzylidenecyclohexane results from both the larger ring size as well as from the chair conformation of the ring which maximizes the steric interaction between the allylic and *ortho* hydrogens.

The current investigation focuses on another  $\beta$ -substituted styrene ring derivative having a smaller four membered ring. The structure of this compound, benzylidenecyclobutane (BCB), is illustrated in Fig. 1. Although the smaller ring leads to smaller steric interactions and therefore might be expected to result in a simpler spectrum, this substitution leads to increased complexity due to the appearance of a number of additional low frequency vibronic modes. Investigation of a deuterated isotopomer of BCB reveals that at least one of these modes has its origins in the low frequency ring puckering motion of the cyclobutane ring. Methylene cyclobutane itself adopts a puckered geometry<sup>17</sup> which undergoes ring inversion over a barrier of  $139 \text{ cm}^{-1}$  at the planar conformation.<sup>18</sup> The fundamental frequency of the puckering mode in methylene cyclobutane has been observed in the far infrared at  $79 \text{ cm}^{-1}$ .<sup>18</sup> When incorporated into the styryl chromophore, the low frequency modes involving phenyl torsion and cyclobutane ring puckering are found to be strongly coupled.

## II. EXPERIMENT

These experiments were performed in a supersonic molecular beam apparatus consisting of two differentially pumped chambers. In the first chamber, maintained at a

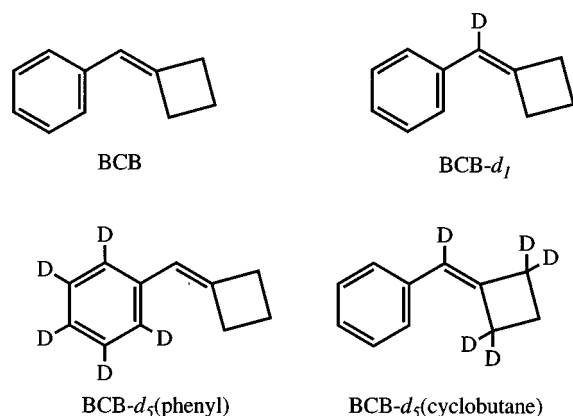


FIG. 1. Structures of the molecules under study: BCB, BCB-*d*<sub>1</sub>, BCB-*d*<sub>5</sub>(phenyl), and BCB-*d*<sub>5</sub>(cyclobutane).

background pressure of approximately 1 mTorr by a 9 in. oil vapor booster pump, the samples, seeded in either He or Ar carrier gas, were expanded from a pulsed nozzle having a 1 mm orifice. The resulting free expansion was skimmed by a 1 mm skimmer producing a molecular beam in the second chamber, which was pumped by a liquid nitrogen trapped 6 in. oil diffusion pump to maintain a base pressure of  $2 \times 10^{-7}$  Torr.

In this second chamber, the molecular beam was crossed in the ionization region of a linear time-of-flight mass spectrometer<sup>19</sup> by an unfocused laser beam from a tunable, frequency doubled, Nd:YAG pumped dye laser. A mixture of rhodamine 590 and rhodamine 610 dyes was used in the dye laser to provide the required range of excitation frequencies, with pulse energies after attenuation of approximately 0.3 mJ. Molecular ions were produced in a one-photon resonant, two-photon ionization process and the mass selected signals were recorded with a gated integrator. When desired, spectra were normalized with respect to variations in the dye laser power by dividing the raw ion signal by the square of the simultaneously recorded laser energy. The squared dependence of the ion signal was established by monitoring the change in the intensity of various vibronic peaks over a range of laser energies. This correction is required for a quantitative analysis of relative peak intensities.

BCB was synthesized according to a procedure described by Bailey *et al.*,<sup>20</sup> in which *n*-BuLi was added to phenylacetylene in THF and then refluxed overnight with diiodopropane. The resulting acetylenic iodide was then cyclized by treatment with *t*-BuLi in *n*-pentane/diethylether at  $-78^\circ\text{C}$  followed by warming to room temperature. Methanol was then added to protonate the vinyl position. Extraction of the organic layer, evaporation of the solvent, and vacuum distillation gave the desired product.

Several deuterated isotopomers of BCB, as illustrated in Fig. 1, were also synthesized during the course of this work. When D<sub>2</sub>O was added instead of methanol at the protonation step in the procedure described above the result was formation of BCB-*d*<sub>1</sub> deuterated at the α position. Syntheses of the

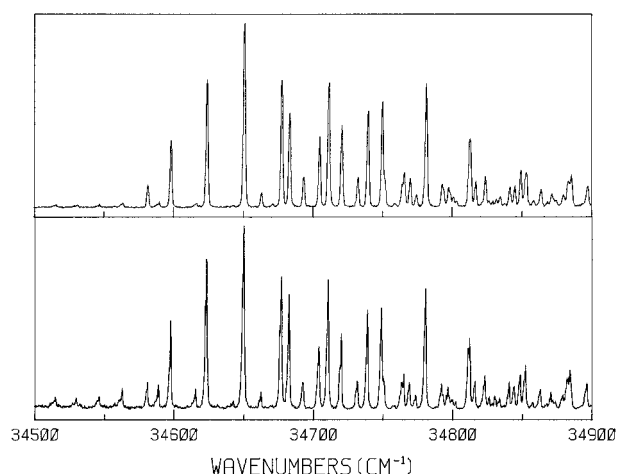


FIG. 2. The resonant two-photon ionization spectrum of BCB expanded in Ar (upper panel) and He (lower panel). The signal was normalized with respect to variation in the dye laser pulse energy.

deuterated derivatives BCB-*d*<sub>5</sub>(phenyl) and BCB-*d*<sub>5</sub>(cyclobutane) were accomplished via Wittig reactions<sup>21</sup> in which the deuterated starting materials were benzyl-*d*<sub>7</sub>-triphenylphosphonium bromide and cyclobutanone-*d*<sub>4</sub>, respectively. The deuterated phosphonium salt was obtained from toluene-*d*<sub>8</sub> in a two-step synthesis, by first refluxing overnight with *N*-bromosuccinimide to yield the fully deuterated benzyl bromide and then reacting the bromide with triphenylphosphine in boiling toluene to give the phosphonium bromide as a white solid in 82% yield. A Wittig reaction with cyclobutanone gave BCB-*d*<sub>5</sub>(phenyl) since the benzylic deuteriums were lost through exchange with protons from the solvent, DMSO. To synthesize BCB-*d*<sub>5</sub>(cyclobutane) the Wittig reaction between cyclobutanone-*d*<sub>4</sub> (obtained from acid catalyzed hydrogen exchange with D<sub>2</sub>O) and triphenylphosphonium bromide was carried out in dimethylsulfoxide-*d*<sub>6</sub> to avoid the exchange of the deuteriums on the cyclobutanone with solvent protons. However, exchange of the benzylic protons in the benzyl-triphenylphosphonium chloride with deuterium from the solvent resulted in formation of the *d*<sub>5</sub> derivative. This procedure avoids the formation of a range of partially deuterated products. The identity of all products was confirmed by GC/MS and <sup>1</sup>H nuclear magnetic resonance spectroscopy.

### III. RESULTS

#### A. Spectrum of BCB

The resonance enhanced photoionization spectrum of BCB is displayed in Fig. 2. The lower panel shows the spectrum observed using an expansion of He at a stagnation pressure of 3.8 atm while the upper panel was obtained using an Ar expansion at 2 atm. Both panels display spectra in which the intensity of the monitored parent ion channel has been normalized to the square of the relative laser energy. The enhanced cooling efficiency of Ar is reflected by the reduction of the hot band intensities in the upper panel. This per-

TABLE I. Observed and calculated torsional energy levels in  $S_1$  and relative intensities in BCB.

$v'$	Torsional spacing ( $\text{cm}^{-1}$ )	Torsional energy ( $\text{cm}^{-1}$ )	Calculated torsional energy ( $\text{cm}^{-1}$ ) <sup>a</sup>	Relative intensity	Calculated relative intensity <sup>b</sup>
0		0.0	0.0	0.14	0.18
1	16.9	16.9	16.9	0.43	0.50
2	25.8	42.7	42.9	0.75	0.77
3	26.6	69.3	69.0	1.00	0.86
4	26.8	96.1	96.1	0.71	0.71
5	27.4	123.5	123.4	0.37	0.45
6	27.2	150.7	150.9	0.17	0.23

<sup>a</sup>Calculated with the optimized parameters  $\nu_0=28.1$ ,  $C=2.43$ ,  $c=0.845$ .

<sup>b</sup>Calculated with the parameters  $S=4.23$ ,  $R=0.812$ .

mits a clear identification of the electronic origin at  $34\,582\text{ cm}^{-1}$ . The weak origin transition is followed within the first  $400\text{ cm}^{-1}$  by a fairly complex pattern of vibronic bands among which several progressions can be identified with spacings on the order of  $27\text{ cm}^{-1}$ . The first such progression is based off the origin and exhibits considerable anharmonicity as revealed by the sudden increase in spacings from  $16.9\text{ cm}^{-1}$  between the first two members to  $25.8\text{ cm}^{-1}$  between the following two. This progression is assigned to the torsional motion of the phenyl ring. A maximum in the intensity distribution is found at the  $v'=3$  level. In Table I the torsional spacings and energy levels in the excited state of BCB are listed for seven members of the progression along with the relative intensities of each transition.

Numerous hot band transitions are also evident in the ionization spectrum recorded with a He expansion. Figure 3 displays the low frequency region of the spectrum, extending to the red of the electronic origin. Several progressions associated with phenyl torsion are observed which can be confidently assigned since the excited state levels are known. Thus transitions from three excited torsional levels of the

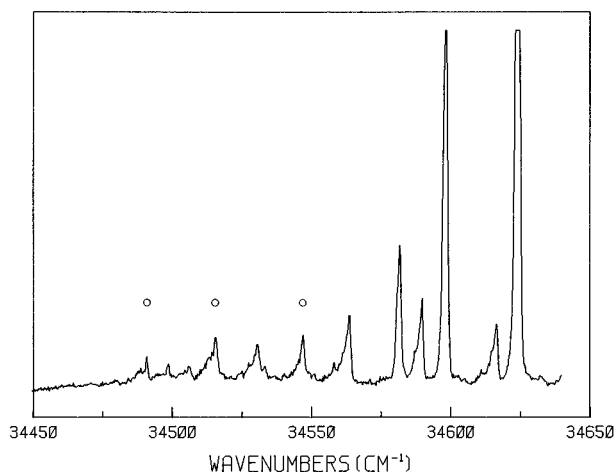


FIG. 3. The low frequency region of the resonant two-photon ionization spectrum of BCB seeded in a He expansion. The origin occurs at  $34\,582\text{ cm}^{-1}$  and three torsional hot bands which terminate on the vibrationless excited state level are marked by circles.

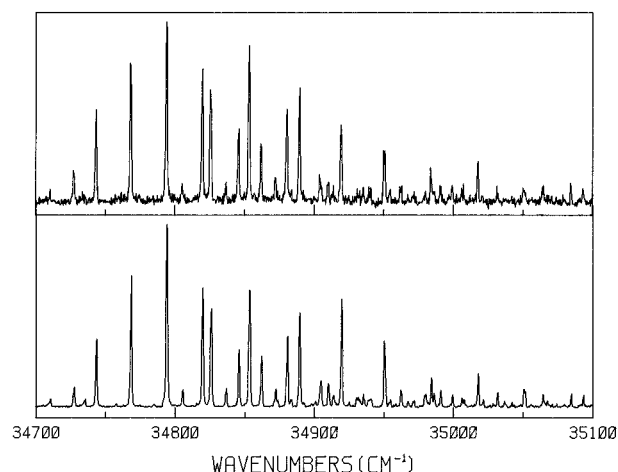


FIG. 4. Resonant two-photon ionization spectrum of BCB- $d_5$ (phenyl) in expansions of Ar (upper panel) and He (lower panel). The plots display the raw ion signal without normalization to the laser energy.

ground state to the vibrationless level of the excited state can be identified at  $34\,547$ ,  $34\,516$ , and  $34\,491\text{ cm}^{-1}$ . This locates these torsional levels in the ground electronic state at  $34.6$ ,  $66.1$ , and  $90.7\text{ cm}^{-1}$ , which yields spacings of  $34.6$ ,  $31.5$ , and  $24.6\text{ cm}^{-1}$ . Again the torsional levels are found to be quite anharmonic, although here displaying spacings which decrease with the torsional quantum number.

Much of the complexity in the spectrum of cold BCB arises from additional torsional progressions which occur in combination with other low frequency fundamental modes. Two such progressions originate  $81.4$  and  $112.1\text{ cm}^{-1}$  above the electronic origin, as seen in Fig. 2. Both of these progressions have different spacings and intensity distributions than the torsional progression based off the origin. For the progression starting at  $81.4\text{ cm}^{-1}$ , the spacing between torsional levels starts at  $20.3\text{ cm}^{-1}$  and increases to  $28.7\text{ cm}^{-1}$ . Torsional levels in combination with the  $112.1\text{ cm}^{-1}$  fundamental exhibit less anharmonicity and show larger spacings.

## B. Spectrum of BCB- $d_5$ (phenyl)

To help confirm the assignment of the torsional progression in the spectrum of BCB, the deuterated isotopomer BCB- $d_5$ (phenyl) was also investigated. This particular isotopic substitution significantly increases the reduced moment of inertia for the phenyl torsion.

The spectrum of BCB- $d_5$ (phenyl) obtained by monitoring the ion signal corresponding to the mass of the pentadeuterated isotopomer is displayed in Fig. 4. Results using both Ar (upper panel) and He (lower panel) expansions are shown. These spectra have not been corrected for variations in the laser energy. The origin transition is located at  $34\,720\text{ cm}^{-1}$ , corresponding to a  $+146\text{ cm}^{-1}$  blueshift. This shift arises from the differential changes in the zero-point vibrational energies of the ground and excited electronic states. The magnitude of the observed shift is roughly comparable to the  $+170\text{ cm}^{-1}$  shift reported by Hui *et al.*<sup>11</sup> for

TABLE II. Observed and calculated torsional energy levels in  $S_1$  of BCB- $d_5$ (phenyl).

$v'$	Torsional spacing ( $\text{cm}^{-1}$ )	Torsional energy ( $\text{cm}^{-1}$ )	Calculated torsional energy ( $\text{cm}^{-1}$ ) <sup>a</sup>	Calculated torsional energy ( $\text{cm}^{-1}$ ) <sup>b</sup>
0		0.0	0.0	0.0
1	16.3	16.3	15.7	16.3
2	24.8	41.1	40.4	41.5
3	25.6	66.7	65.1	66.5
4	26.0	92.7	90.8	92.4
5	25.7	118.4	116.7	118.5
6	26.4	144.8	142.8	144.9

<sup>a</sup>Calculated with the isotopically adjusted parameters  $\nu_0=26.7$ ,  $C=2.55$ ,  $c=0.805$ .

<sup>b</sup>Calculated with the optimized parameters  $\nu_0=26.9$ ,  $C=2.38$ ,  $c=0.887$ .

styrene- $d_8$ , relative to the undeuterated species, as well as to the value of  $+131 \text{ cm}^{-1}$  found upon deuteration of the benzene ring in 1-phenyl-1,3-butadiene.<sup>22</sup>

Except for the slight changes in the torsional spacings the spectrum appears quite similar to that of the undeuterated compound. The main torsional progression based off the origin exhibits initial spacings of  $16.3$  and  $24.8 \text{ cm}^{-1}$  which then stay fairly constant at approximately  $26 \text{ cm}^{-1}$ . The intensity pattern among the peaks in this progression is not significantly altered by the deuteration, peaking again at the  $v'=3$  level. Table II lists the observed torsional energies and spacings in the excited electronic state. Similarly, torsional levels in the ground electronic state from which transitions to the vibrationless excited state occur were identified in the spectrum taken in a He expansion to yield values of  $33.2$ ,  $64.0$ , and  $88.0 \text{ cm}^{-1}$  for the three lowest levels.

Two additional torsional progressions are also identified with origins  $77.7$  and  $109.2 \text{ cm}^{-1}$  above the electronic origin. Thus deuteration of the benzene ring induces a shift of  $-3.8$  and  $-2.9 \text{ cm}^{-1}$ , respectively, in the fundamentals on which these progressions are based. The torsional spacings in the second progression show a large initial increase from  $20.7 \text{ cm}^{-1}$  between the first and second members to  $27.7 \text{ cm}^{-1}$  between the second and third. The corresponding levels based off the  $109.2 \text{ cm}^{-1}$  vibration exhibit a smaller degree of anharmonicity. Although the intensity distributions within each of the three torsional progressions are quite different, they remain unchanged from what is seen in the undeuterated compound.

### C. Spectrum of BCB- $d_5$ (cyclobutane)

A second isotopomer investigated was BCB- $d_5$ (cyclobutane) in which the four allylic positions on the cyclobutane ring were deuterated as well as the  $\alpha$  position on the vinyl group. The  $\alpha$  deuteration was required to permit the synthesis of an isotopically pure sample. This is necessary, despite the fact that the mass spectrometer can readily distinguish molecules differing by 1 amu, because it is difficult in a spectral scan to prevent the signal from such a species from leaking into the desired mass channel. That this pentadeuterated isotopomer is representative of BCB

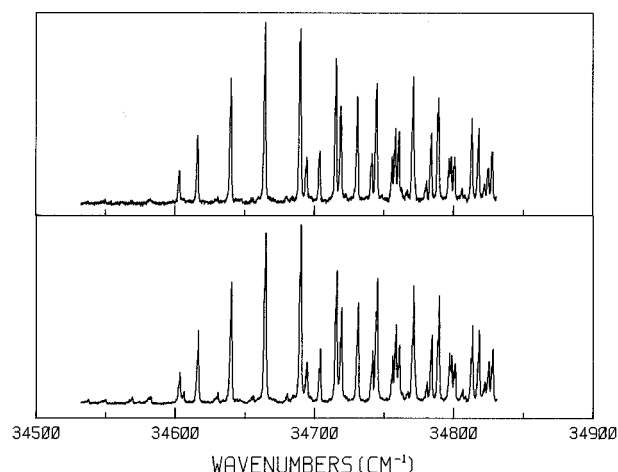


FIG. 5. Resonant two-photon ionization spectrum of BCB- $d_5$ (cyclobutane) in expansions of Ar (upper panel) and He (lower panel). The plots display the raw ion signal without normalization to the laser energy.

deuterated only on the cyclobutane ring was confirmed by studies on BCB- $d_1$  which is deuterated only at the  $\alpha$  position. The photoionization spectrum of this species was found virtually indistinguishable from that of the undeuterated molecule. Deuteration of the cyclobutane ring modifies the effective masses of both the torsional mode as well as any modes derived from the cyclobutane ring which involve considerable motion of the allylic hydrogens.

The mass resolved resonant two-photon ionization spectrum of BCB- $d_5$ (cyclobutane) is shown in Fig. 5 in both He and Ar expansions. The electronic origin is found at  $34604 \text{ cm}^{-1}$ , corresponding to a small,  $+22 \text{ cm}^{-1}$ , shift upon deuteration of the cyclobutane ring. This is similar to the findings for styrene<sup>2,11</sup> and 3-methyl- $d_3$ -styrene<sup>7</sup> when deuteration is performed away from the benzene ring. Unlike the previous case of BCB- $d_5$ (phenyl), this deuteration results in a pattern of vibronic transitions that is markedly different from the undeuterated species. First, a large change in the spacings within the torsional progression based off the electronic origin is observed. The first torsional interval is only  $13.1 \text{ cm}^{-1}$ , which is  $3.8 \text{ cm}^{-1}$  smaller than in BCB and  $3.2 \text{ cm}^{-1}$  smaller than in BCB- $d_5$ (phenyl). Subsequent spacings increase to  $23.9$  and  $24.6 \text{ cm}^{-1}$  then approach a value of  $25.5 \text{ cm}^{-1}$ . The observed torsional levels are listed in Table III. The three lowest torsional levels in the ground electronic state with transitions to the vibrationless level of the excited electronic state are found at  $34.5$ ,  $66.0$ , and  $91.9 \text{ cm}^{-1}$ .

Significant differences are also evident in the torsional progressions based off the two other fundamental vibrational modes. The first fundamental is found at  $91.4 \text{ cm}^{-1}$ , corresponding to a  $10.0 \text{ cm}^{-1}$  shift to higher frequency, relative to BCB, while the second appears at  $100.8 \text{ cm}^{-1}$ , representing a shift of  $11.3 \text{ cm}^{-1}$  to lower frequency. In the phenyl deuterated species these two transitions both underwent much smaller shifts on the order of  $3 \text{ cm}^{-1}$  and in both cases to smaller frequencies. Torsional levels in combination with both of these vibrations exhibit spacings which are substan-

TABLE III. Observed and calculated torsional energy levels in  $S_1$  of BCB- $d_5$ (cyclobutane).

$v'$	Torsional spacing ( $\text{cm}^{-1}$ )	Torsional energy ( $\text{cm}^{-1}$ )	Calculated torsional energy ( $\text{cm}^{-1}$ ) <sup>a</sup>	Calculated torsional energy ( $\text{cm}^{-1}$ ) <sup>b</sup>
0		0.0	0.0	0.0
1	13.1	13.1	15.7	13.1
2	23.9	37.0	40.3	37.5
3	24.6	61.6	64.9	61.4
4	25.4	87.0	90.5	86.7
5	25.5	112.5	116.4	112.4
6	25.7	138.2	142.5	138.4

<sup>a</sup>Calculated with the isotopically adjusted parameters  $\nu_0=26.7$ ,  $C=2.56$ ,  $c=0.804$ .

<sup>b</sup>Calculated with the optimized parameters  $\nu_0=26.8$ ,  $C=3.31$ ,  $c=0.725$ .

tially different from their respective values in both BCB and BCB- $d_5$ (phenyl). The relative intensities of these combination bands also deviate from the two previous derivatives. The second progression appears more extended than in BCB while the third shows the opposite trend.

## IV. DISCUSSION

### A. One-dimensional torsional analysis

#### 1. Excited state levels

As a starting point for understanding the torsional motion in BCB, a one-dimensional analysis of the origin-based torsional progressions in each of the three isotopomers was undertaken. Large amplitude hindered rotations are typically treated with a Hamiltonian of the following form:<sup>23</sup>

$$H = -B \frac{d^2}{d\tau^2} + V(\tau), \quad (1)$$

where  $B$  represents the reduced rotational constant for torsion and  $V(\tau)$  is the potential energy expressed as a function of the torsional angle  $\tau$ . The periodic torsional potential is commonly written as a Fourier cosine expansion:

$$V(\tau) = \frac{1}{2} \sum_n V_n (1 - \cos n\tau). \quad (2)$$

Attempts to model the excited state torsional potential in BCB were carried out using  $V_2$ ,  $V_4$ , and  $V_6$  terms since the twofold symmetry of the phenyl rotor requires only even  $n$  terms be retained in the expansion. The reduced rotational constant,  $B$ , is inversely proportional to the reduced moment of inertia for the internal rotation,  $I_r$ , which was calculated using the formulation of Pitzer<sup>24</sup> applicable to balanced rotors. This requires a knowledge of the molecular structure in the excited electronic state, which was estimated using a semiempirical configuration-interaction calculation with the AM1 Hamiltonian as contained in MOPAC ver. 5.00.<sup>25</sup> The resulting equilibrium structure was determined to have  $C_s$  symmetry, with all carbon atoms lying in a common plane. From this structure a value of 43.4 amu  $\text{\AA}^2$  was determined for  $I_r$  leading to a value of 0.388  $\text{cm}^{-1}$  for  $B$ .

Eigenvalues of the hindered rotor Hamiltonian, Eq. (1), were calculated in a variational approach, making use of a free-rotor basis set,<sup>26</sup> and the potential parameters  $V_2$ ,  $V_4$ , and  $V_6$  were varied in a nonlinear least-squares procedure to optimize the fit between the calculated eigenvalues and the observed torsional levels in the excited electronic state. A fit using only these three parameters was unable to reproduce experimental values, particularly the unusual spacings between the three lowest levels, to better than several wave numbers. The torsional potential must be quite flat at the bottom of the well and this behavior is difficult to accurately model with a three parameter cosine expansion.

As an alternative to the cosine expansion of the torsional potential, Eq. (2), a quadratic + Gaussian potential was investigated as a means to better reproduce the flat-bottomed well without requiring a large number of parameters. This potential has the form:

$$V(\tau) = \frac{1}{2}k\tau^2 + A \exp(-a\tau^2) \quad (3)$$

and is clearly an approximation valid only in the region of the potential minimum since it is not periodic. Nevertheless, it is capable of producing flat-bottom or double minimum wells, depending on the magnitudes of the parameters  $k$ ,  $A$ , and  $a$ . With this potential, the hindered rotor Hamiltonian can be recast from Eqs. (1) and (3) using the dimensionless normal coordinate  $Q$  as:

$$H = \frac{\nu_0}{2} \left[ -\frac{d^2}{dQ^2} + Q^2 + C \exp(-cQ^2) \right]. \quad (4)$$

The correlation between  $\tau$  and  $Q$  and the corresponding transformations between the equivalent sets of potential parameters are given below:

$$\tau = \sqrt{\frac{2B}{\nu_0}} Q, \quad k = \frac{\nu_0^2}{2B}, \quad A = C \frac{\nu_0}{2}, \quad a = c \frac{\nu_0}{2B}. \quad (5)$$

The eigenvalues of the Hamiltonian in Eq. (4) were determined in a variational approach using the method of Coon, Naugle, and McKenzie<sup>27</sup> with separate basis sets of 50 harmonic oscillator wave functions of even or odd symmetry of frequency  $\nu_0$ . A nonlinear least-squares fit to the observed torsional levels in BCB performed on  $\nu_0$ ,  $C$ , and  $c$  yields values of 28.1  $\text{cm}^{-1}$ , 2.43, and 0.845, respectively. These values result in the calculated torsional energy levels displayed in the fourth column of Table I which are found to differ by at most 0.3  $\text{cm}^{-1}$  from the experimental observations. In combination with the value of the reduced rotational constant,  $B$ , the torsional potential in Eq. (3) becomes fully defined and is plotted in Fig. 6. This potential surface displays two minima at  $\pm 8.7^\circ$ , separated by a barrier at  $0^\circ$  of 5.5  $\text{cm}^{-1}$ . The ground torsional level lies 3.4  $\text{cm}^{-1}$  above this barrier, leading to a planar equilibrium structure which undergoes large amplitude torsional motion.

Deuteration of BCB results in different values of  $I_r$  and hence  $B$ , but the potential parameters  $k$ ,  $A$ , and  $a$  extracted from  $\nu_0$ ,  $C$ ,  $c$ , and  $B$  of the undeuterated species via Eq. (5) should remain unchanged if the one-dimensional analysis is correct. The analysis of the torsional levels in

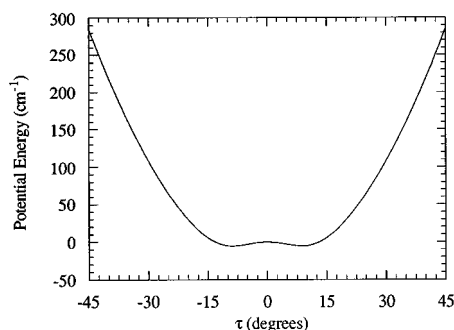


FIG. 6. Excited state torsional potential of BCB, calculated with Eq. (3) after optimizing the potential parameters to fit the observed energy levels.

BCB- $d_5$ (phenyl) was therefore performed in two ways. First, new values of  $\nu_0$ ,  $C$ , and  $c$  were recalculated from those obtained from the optimized fit on BCB after determining the value of the reduced rotational constant,  $B$ , to be  $0.352 \text{ cm}^{-1}$  from the same excited state structure used previously. This results in values of  $26.7 \text{ cm}^{-1}$ ,  $2.55$ , and  $0.805$  for  $\nu_0$ ,  $C$ , and  $c$ . The energy levels resulting from these parameters are shown in the fourth column of Table II and are seen to reproduce the experimental values to within  $2 \text{ cm}^{-1}$ . A complete reoptimization of the potential parameters yields values of  $26.9 \text{ cm}^{-1}$ ,  $2.38$ , and  $0.887$  for  $\nu_0$ ,  $C$ , and  $c$  and predicts torsional levels to within  $0.4 \text{ cm}^{-1}$  as shown in the fifth column of Table II. The small differences between these two sets of parameters [the two plots of  $V(\tau)$  are essentially indistinguishable] give no indication that the one-dimensional treatment is not valid.

However, when the same double analysis is repeated on BCB- $d_5$ (cyclobutane) the agreement between the two approaches breaks down. A reevaluation of the reduced moment of inertia for cyclobutane deuteration yields a value of  $0.351$  for  $B$ , resulting in values of  $26.7 \text{ cm}^{-1}$ ,  $2.56$ , and  $0.804$  for  $\nu_0$ ,  $C$ , and  $c$  using Eq. (5) and the parameters from the undeuterated species. These parameters give a poor representation of the observed torsional levels, as illustrated in the fourth column of Table III. Nevertheless a full optimization procedure is able to accurately reproduce experiment, as shown in the fifth column, using values of  $26.8 \text{ cm}^{-1}$ ,  $3.31$ , and  $0.725$  for the potential parameters  $\nu_0$ ,  $C$ , and  $c$ . Note that a considerable change in the values of both the  $C$  and  $c$  parameters is required, resulting in torsional potentials with different locations of the minima and different barrier heights. This observation will be shown to be indicative of a mixing of the torsion with other vibrational modes.

## 2. Franck-Condon analysis

Information about the ground state torsional surface arises from two sources in the resonant ionization spectrum of BCB. Ground state torsional levels are observed directly in the weak hot band region of the spectrum and these will be discussed later. Additionally, the intensity distribution of the excited state torsional progression is sensitive to the nature of the ground state surface, particularly the location of

the potential minimum. In order to support the extended progression in the torsional mode, the ground state minimum must be substantially displaced from a  $C_s$  symmetry ( $\tau=0^\circ$ ) excited state. To interpret the torsional intensities the simplest approximation is employed, in which it is assumed that the lowest ground state torsional wave function can be well modeled by the ground state of a harmonic oscillator having a frequency of  $34.6 \text{ cm}^{-1}$ , corresponding to the spacing between the ground and first excited torsional levels extracted from the hot band analysis.

Within this approximation, the vibrational overlap integrals between this displaced ground state oscillator and various torsional wave functions in the excited electronic state are readily evaluated since the excited state wave functions have already been expressed in a basis set of harmonic oscillators of frequency  $\nu_0$ , centered at  $\tau=0^\circ$ . Therefore the overlap of the ground torsional level with any torsional level in the excited state was calculated as a sum of the products between the previously determined expansion coefficients and harmonic oscillator overlap integrals. The overlap integrals are most conveniently evaluated in terms of two parameters:  $R = \nu_e/\nu_g$ , the ratio of the frequencies of the two oscillators, and  $S$ , a measure of the displacement,  $\Delta\tau$ , between the two potential minima.<sup>28</sup> With  $R$  fixed at  $28.1/34.6 = 0.812$ ,  $S$  was varied in a nonlinear least-squares procedure to fit the relative intensities in the excited state torsional progression of BCB (the fifth column of Table I). Optimization resulted in a value of  $4.23$  for  $S$  and produced the calculated relative intensities also shown in Table I. Having determined  $S$ , the torsional displacement  $\Delta\tau$  is given by:

$$(\Delta\tau)^2 = 4(B/\nu_g)S, \quad (6)$$

which yields a value of  $0.431 \text{ rad}$  or  $24.7^\circ$  for  $\Delta\tau$ . The value of the ground state rotational constant in Eq. (6) was estimated at  $0.380 \text{ cm}^{-1}$  from a ground state *ab initio* geometry optimization performed at the Hartree-Fock level with a 3-21G basis set.<sup>29</sup> Since the excited state torsional levels are expressed in harmonic oscillator wave functions centered at  $\tau=0^\circ$  this result implies a ground state torsional geometry in which the vinyl group is twisted  $25^\circ$  out of the plane of the phenyl ring.

## 3. Ground state levels

With evidence that the vinyl group does not lie in the phenyl ring plane in the ground electronic state of BCB, the possibility of at least two conformations arises since torsion out of the plane can occur in two directions and the cyclobutane ring may not be planar. However, two pieces of evidence argue against this conclusion. First there are no distinct spectral lines in the resonantly enhanced ionization spectrum that appear to require a second ground state conformer. Additional evidence for the lack of a second ground state conformer is provided by the behavior of the observed spectrum as the laser pulse energy is increased. As saturating conditions are approached the lines with the stronger Franck-Condon factors saturate first allowing the weaker transitions to grow in relative intensity. Eventually lines

saturate to a value determined by the population of the lower level of the transition. This procedure has previously been used to identify different conformations in the ground electronic states of several tryptophan derivatives<sup>30</sup> as well as of a phenyl substituted retinyl polyene.<sup>31</sup> In the case of BCB, these saturation experiments were carried out over a wide range of pulse energies and gave no indication that different sets of lines were saturating to different levels.

The fact that there is no spectral evidence for a second ground state conformer, coupled with the conclusion that the ground state geometry has a nonzero torsional angle, requires a symmetric double-well torsional potential where torsion in the opposite direction produces a spectroscopically equivalent conformation. If this is the case and the barrier between the two wells is small, the ground state torsional levels will split into symmetric (+) and antisymmetric (-) components. Since the excited state potential was found centered at the  $C_s$  geometry, torsional levels with even quanta of excitation are symmetric and levels with odd quanta of excitation are antisymmetric. Vibronic transitions between symmetric and antisymmetric levels are forbidden so all transitions which terminate on excited state levels with even quanta must originate from the symmetric component of the ground state level while all transitions which terminate on excited state levels with odd quanta must originate from the antisymmetric component of the ground state level.

This requires that a more careful analysis of the hot band region of the spectrum be performed so that both symmetric and antisymmetric components of the ground state torsional levels can be identified. The symmetric components are readily assigned using hot band transitions that terminate on the vibrationless excited state level through

$$T_{v+} = T_{0+}^0 - T_{v+}^0, \quad (7)$$

where  $T_{v+}$  represents the torsional energy of the symmetric component of the  $v$ th level in the ground electronic state and  $T_{0+}^0 - T_{v+}^0$  gives the measured energy difference between the electronic origin and the hot band originating from the  $v+$  level. Alternatively, the antisymmetric components are assigned using hot band transitions which terminate on the first excited torsional level in the excited electronic state through

$$T_{v-} = (T_{0-}^1 - T_{v-}^1) + (T_{0-} - T_{0+}), \quad (8)$$

where  $T_{v-}$  represents the energy of the antisymmetric component of the  $v$ th ground state torsional level,  $T_{0-}^1 - T_{v-}^1$  gives the measured energy difference between the torsional transitions that terminate on the first excited level in the excited state, and  $T_{0-} - T_{0+}$  gives the splitting between the two components of the  $v=0$  level in the ground electronic state. The splitting between the  $0+$  and  $0-$  levels cannot be directly observed but in this treatment is assumed to be negligibly small. The torsional levels in the ground electronic state calculated in this fashion are listed in column 2 of Table IV. Note that no splitting is resolved in the  $v=1$  level but that a small  $1.3 \text{ cm}^{-1}$  splitting is observed in the  $v=2$  level. Characterization of these levels and splittings is hampered somewhat by the larger rotational band contours associated with these thermally excited levels.

TABLE IV. Observed and calculated torsional energy levels in  $S_0$  of BCB.

$v''$	Torsional energy ( $\text{cm}^{-1}$ )	Calculated torsional energy ( $\text{cm}^{-1}$ ) <sup>a</sup>	<i>Ab initio</i> torsional energy ( $\text{cm}^{-1}$ ) <sup>b</sup>
0+	0.0	0.0	0.0
0-	0.0 <sup>c</sup>	0.002	0.008
1+	34.6	34.7	37.3
1-	34.6	34.8	37.6
2+	66.1	66.0	69.5
2-	67.4	67.3	72.6
3+	90.7	90.7	94.9
3-		98.3	106.9

<sup>a</sup>Calculated with the optimized parameters  $\nu_0=21.8$ ,  $C=23.9$ ,  $c=0.176$ .

<sup>b</sup>Calculated from a fit to the *ab initio* potential with the parameters  $\nu_0=23.7$ ,  $C=21.2$ ,  $c=0.200$ .

<sup>c</sup>The splitting between  $0-$  and  $0+$  cannot be directly measured but is assumed to be negligible.

The ground state levels in Table IV can also be fit to a quadratic+Gaussian potential as done previously for the excited state. A nonlinear least-squares fit found optimal values for the potential parameters of  $\nu_0=21.8 \text{ cm}^{-1}$ ,  $C=23.9$ , and  $c=0.176$ . These parameters generate the torsional potential shown in Fig. 7 as a solid line. This potential exhibits two equivalent minima at  $\tau=\pm 29.6^\circ$  with a barrier at  $\tau=0^\circ$  of  $109 \text{ cm}^{-1}$ . The energy levels predicted by this potential are given in the third column of Table IV and are seen to differ by at most  $0.2 \text{ cm}^{-1}$  from experiment. Note that splittings predicted for the  $v=0$  and  $v=1$  levels are only  $0.002$  and  $0.1 \text{ cm}^{-1}$ , which are both much smaller than the rotational contours of the transitions used to make the assignments.

Upon deuteration the rotational constants,  $B$ , for BCB- $d_5$ (phenyl) and BCB- $d_5$ (cyclobutane) in the ground electronic state decrease to  $0.343$  and  $0.347 \text{ cm}^{-1}$ , respectively. Due to the similarity in these values only negligible differences in the ground state torsional levels would be predicted. However an analysis of the hot band region of the spectrum of these two species reveals that the level spacings in BCB- $d_5$ (phenyl) decrease relative to BCB, as expected, but that in BCB- $d_5$ (cyclobutane) very little change is ob-

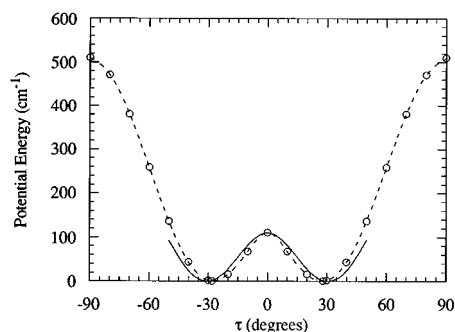


FIG. 7. Ground state torsional potential of BCB (solid line) obtained by fitting the experimental ground state energies to the quadratic+Gaussian potential in Eq. (3). The dotted line represents *ab initio* results from calculations at the Hartree-Fock 3-21G level in which the torsional angle was varied in  $10^\circ$  increments and all other degrees of freedom were unconstrained.



served upon deuteration. This anomalous behavior of the torsional levels in the cyclobutane deuterated species mirrors what was seen in the excited electronic state, demonstrating that the source of this effect is present in both electronic states.

## B. *Ab initio* calculations

To investigate the symmetric double-well nature of the ground state torsional potential, a series of *ab initio* geometry optimizations was carried out at fixed  $10^\circ$  torsional intervals using the 3-21G basis set. The remaining degrees of freedom in the molecule were allowed to vary to locate the energy minimum. The potential thus obtained is displayed in Fig. 7 as a dotted line in comparison to the potential obtained from the earlier analysis of the torsional hot bands. It is clearly seen to be symmetric about the fully conjugated conformation with two potential minima located at  $\tau = \pm 28^\circ$  which are separated by a barrier of  $110 \text{ cm}^{-1}$ . Such a potential can also be very accurately reproduced by a quadratic +Gaussian function as discussed earlier with parameter values of  $\nu_0 = 23.7 \text{ cm}^{-1}$ ,  $C = 21.2$ , and  $c = 0.200$  chosen to provide the optimal fit. These parameters can subsequently be used to predict ground state torsional levels as are given in the fourth column of Table IV. While the calculated values are consistently larger than those observed experimentally, they do provide fairly reasonable estimates of the torsional energies thus lending support to the calculated surface.

Examination of the calculated structures at the potential minima shows that the two are simply mirror image conformations involving phenyl torsion and cyclobutane ring puckering in the opposite direction. This is consistent with the results from the saturation experiments. At the top of the torsional barrier, a  $C_s$  symmetry structure is predicted indicating that motion along this coordinate involves both torsion of the phenyl ring and inversion of the cyclobutane ring. Unlike the case of benzylidencyclopentane, which also exhibits two mirror image conformations,<sup>15,16</sup> motion along this adiabatic torsional coordinate results in conformer interconversion over a very low energy barrier.

The fact that the transition state at  $\tau = 0^\circ$  for conformer interconversion is predicted to have a planar cyclobutane ring lends support to the assignment of a  $C_s$  symmetry structure to the excited state. When the torsion angle approaches  $0^\circ$ , whether in passing over the torsional barrier in the ground electronic state or in the equilibrium conformation of the excited electronic state, the cyclobutane ring appears to have sufficient flexibility to distort in a manner to reduce the steric interactions of the two allylic hydrogens with the phenyl *ortho* hydrogen. In a planar ring conformation the steric interaction is distributed equally between the two allylic hydrogens.

Fully optimized geometries were also obtained at the *ab initio* Hartree–Fock level with both 3-21G and 6-31G\* basis sets<sup>29</sup> and the results of the latter are displayed in Fig. 8. In conjunction with a  $28^\circ$  phenyl torsion angle, the cyclobutane ring in BCB was calculated, with a 3-21G basis, to adopt a conformation with a ring-puckering angle of  $17^\circ$ . This angle

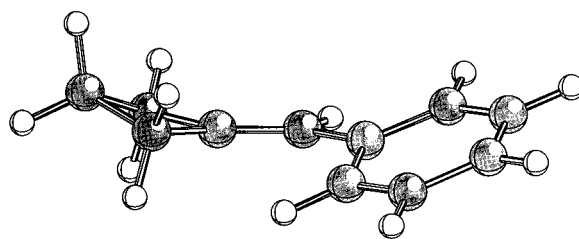


FIG. 8. Ground state BCB structure obtained from an *ab initio* Hartree–Fock geometry optimization using a 6-31G\* basis set.

is defined as the angle between the planes which contain the three carbon atoms on either side of the puckered ring. The higher level 6-31G\* calculation was performed as a check on the accuracy of the 3-21G predictions and yielded very similar torsion and ring-puckering angles, with values of  $26^\circ$  and  $19^\circ$ , respectively.

A  $19^\circ$  puckering angle is very similar to the  $22^\circ$  value derived for the cyclobutane ring in methylenecyclobutane, MCB, from a combination of electron diffraction and microwave data.<sup>32</sup> The calculated  $110 \text{ cm}^{-1}$  barrier for conformer interconversion in BCB is slightly lower than the  $139 \text{ cm}^{-1}$  barrier in MCB<sup>18</sup> indicating that the  $C_s$  symmetry transition state in the former is stabilized by conjugation with the phenyl ring.

## C. Torsional coupling

The one-dimensional analyses of the origin-based torsional progressions in the spectra of BCB and its two isotopomers were made assuming that this motion corresponded to rigid torsion of the phenyl group about the single bond connecting it to the methylenecyclobutane ring. While this picture does permit the spectra of both the undeuterated and the phenyl ring deuterated species to be fit using a common set of potential parameters, these same parameters do not adequately reproduce the observed torsional levels in the cyclobutane ring deuterated species, BCB- $d_5$ (cyclobutane). Since the multidimensional molecular potential energy surface must be invariant to isotopic substitution, this observation requires a more careful investigation of the molecular motion assigned to the torsional mode. One cause of the observed discrepancy may be the assumption of a rigid torsional motion which does not include any simultaneous variation of the puckering angle of the cyclobutane ring. The inclusion of this motion would slightly modify the effective masses, appearing as reduced moments of inertia, of the torsional mode from the values used earlier. Since the ground electronic state adopts a conformation with nonzero values for both the torsional angle and the ring puckering angle it appears plausible that the observed low frequency mode in the excitation spectra contains contribution from both the torsion and puckering motions. A reevaluation of the effective masses might then give a new set of values which in combination with a single set of potential parameters would accurately reproduce the observed torsional levels in all three isotopic species.

The effective mass for the combined torsion–puckering motion was calculated using a one-dimensional reduction of the Wilson  $G$  matrix formalism<sup>33</sup> as

$$m_{\text{eff}} = \sum_i m_i \left( \frac{dr_i}{d\tau} \right)^2, \quad (9)$$

where  $dr_i$  is the change in the coordinate vector of the  $i$ th atom which occurs for a corresponding change  $d\tau$  in the torsional angle. The motion comprising this mode is defined so that a  $3.3^\circ$  change in the torsional coordinate  $\tau$  away from the equilibrium value of  $0^\circ$  is accompanied by a  $2.0^\circ$  pucker of the cyclobutane ring. This ratio of torsion to pucker was chosen since it will transform a planar structure, as found in the excited state, into one having the torsion and puckering angles calculated for the ground electronic state.

A semirigid bisector model was used to describe the motion of the four-membered ring. This model was first introduced by Chan *et al.*<sup>34</sup> for trimethylene oxide and was later applied to cyclobutane<sup>35</sup> and other pseudo-four-membered ring molecules.<sup>36</sup> In this model the methylenecyclobutane ring folds about the ring diagonal such that all bond distances remain constant. Concomitant motion of the hydrogen atoms attached to the methylene groups about which folding occurs preserves the HCH bond angles and keeps the bisectors of both the HCH bond angles and the interior ring bond angles coincident throughout the vibration. Using an optimized molecular geometry calculated at the AM1 level and subject to the bisector model constraints, the Cartesian coordinates of each atom in BCB were computed first for the equilibrium planar structure and then for a structure having a torsional angle of  $3.3^\circ$  and a puckering angle of  $2.0^\circ$ . This procedure was facilitated using the vector representation of Laane *et al.*<sup>37</sup> The two sets of Cartesian coordinates were then both converted to the principal moment of inertia frame to remove any contributions from translational and rotational motion and their difference used to represent the differential changes  $dr_i$  which, in combination with a value of  $3.3^\circ$  for  $d\tau$ , were used to estimate the effective mass of this vibrational mode via Eq. (9).

The above procedure leads to an effective mass in the form of a reduced moment of inertia of  $61.0 \text{ amu } \text{\AA}^2$  for the undeuterated species and to values of  $66.4$  and  $66.7 \text{ amu } \text{\AA}^2$  for the phenyl and the cyclobutane deuterated species, respectively. With these values the observed torsional levels in BCB and BCB- $d_5$ (phenyl) can once again be quite reasonably fit by a single set of potential parameters but the case of BCB- $d_5$ (cyclobutane) again proves problematic. This is readily apparent from the nearly identical calculated values of the effective masses of the two deuterated species which nevertheless exhibit quite different torsional levels. Therefore inclusion of additional ring puckering motion into the torsional normal coordinate fails to provide an adequate description of the experimental results.

An alternative explanation for the observed discrepancy is that deuteration of the cyclobutane ring results in substantial mixing of the excited state normal modes relative to those in the excited states of the undeuterated and phenyl

deuterated species. Strong support for this second explanation can be found by comparing the frequencies of the two other low frequency fundamentals found in the spectra of all three species. In BCB these fundamentals are seen at  $81.4$  and  $112.1 \text{ cm}^{-1}$  and are observed to shift to lower frequencies of  $77.7$  and  $109.2 \text{ cm}^{-1}$  following phenyl deuteration in BCB- $d_5$ (phenyl). However in BCB- $d_5$ (cyclobutane) the lower frequency mode shifts to a higher frequency of  $91.4 \text{ cm}^{-1}$  while the higher frequency mode shifts to a lower frequency of  $100.8 \text{ cm}^{-1}$ . The very large magnitudes of these shifts and the shift to higher frequency cannot be explained solely in terms of a change in the effective mass of a single normal coordinate that occurs upon deuteration. Instead this is taken as evidence of mixing the normal modes of BCB- $d_5$ (cyclobutane) relative to those in the undeuterated species. The mixing may also include, to a lesser extent, the mode formally labeled as torsion if all have the same symmetry. Inclusion of this mode in the mixing would readily account for the breakdown of the earlier one-dimensional analyses and require at minimum a three-dimensional model.

To more closely examine this hypothesis, ground state harmonic frequencies were calculated at the *ab initio* Hartree–Fock level using a 3-21G basis set. Four frequencies were found with values less than  $140 \text{ cm}^{-1}$  and were assigned by visualization of the normal modes. A frequency of  $36 \text{ cm}^{-1}$  was found for the torsional mode while frequencies of  $101$  and  $118 \text{ cm}^{-1}$  were assigned to the cyclobutane ring puckering and the out-of-plane bend of the vinyl group, respectively. The fourth mode at  $139 \text{ cm}^{-1}$  was found to correspond to an in-plane bend about the  $\alpha$  vinyl carbon. Since the ground state geometry of BCB is not planar, the distinction between in-plane and out-of-plane modes is not rigorous, but in an excited state of  $C_s$  symmetry all in-plane modes would have  $A'$  symmetry and all out-of-plane modes would have  $A''$  symmetry. Thus the proposed normal mode mixing appears to involve the three low frequency  $A''$  modes corresponding to torsion, ring puckering, and out-of-plane bending.

Spectroscopic evidence for mode mixing in styrene has previously been observed and carefully detailed in the work of Hollas *et al.*<sup>2–4</sup> Here the ground state normal modes corresponding to torsion at  $38 \text{ cm}^{-1}$  and out-of-plane bending at  $199 \text{ cm}^{-1}$  become heavily mixed in the lowest excited singlet state where their frequencies undergo a substantial shift to  $102$  and  $191 \text{ cm}^{-1}$ . Confirmation of mode mixing as the origin of this effect was provided by single vibronic level fluorescence spectroscopy. Deuteration of styrene at the  $\beta$  carbon was also found to slightly alter the extent of the mixing. These same two modes, together with ring puckering, are proposed to be strongly mixed in BCB- $d_5$ (cyclobutane) although here the origin of the effect arises from a change in the effective masses following selective deuteration rather than a change in the force constants associated with electronic excitation.

## V. CONCLUSION

Electronic spectroscopy has been used to characterize the ground and first singlet excited states of benzylidenecy-

clobutane. The observed torsional energy levels in the parent compound as well as two deuterated isotopomers can each be accurately reproduced by one-dimensional potential energy functions which lead to essentially planar excited state conformations that undergo large amplitude motion and ground state conformations with torsional angles of  $\sim 25^\circ$  and puckered cyclobutane rings. These findings for the ground state are consistent with *ab initio* Hartree–Fock calculations. Although multiple minima are found on the ground state potential energy surface they correspond to equivalent mirror image conformations which are readily interconverted over low energy barriers.

Although the spectrum of each isotopomer could be accurately reproduced by one-dimensional analysis, a common set of potential parameters could not be found that would adequately reproduce the observed torsional levels of all three species. This is taken as evidence for mixing of the torsional mode with other low frequency modes of the same symmetry. These include the cyclobutane ring puckering and the vinyl group out-of-plane bend. The extent of the mixing varies with isotopic substitution and is considerably different in the cyclobutane deuterated derivative than in the phenyl deuterated and undeuterated species.

- <sup>1</sup>D. A. Condirston and J. D. Lapos, *J. Mol. Spectrosc.* **63**, 466 (1976).  
<sup>2</sup>J. M. Hollas, E. Khalilipour, and S. N. Thakur, *J. Mol. Spectrosc.* **73**, 240 (1978).  
<sup>3</sup>J. M. Hollas and T. Ridley, *Chem. Phys. Lett.* **89**, 232 (1981).  
<sup>4</sup>J. M. Hollas, H. Musa, T. Ridley, P. H. Turner, and K. H. Weisenberger, *J. Mol. Spectrosc.* **94**, 437 (1982).  
<sup>5</sup>W. Caminati, B. Vogelsanger, and A. Bauder, *J. Mol. Spectrosc.* **128**, 384 (1988).  
<sup>6</sup>J. I. Seeman, V. H. Grassian, and E. R. Bernstein, *J. Am. Chem. Soc.* **110**, 8542 (1988).  
<sup>7</sup>V. H. Grassian, E. R. Bernstein, H. V. Secor, and J. I. Seeman, *J. Phys. Chem.* **93**, 3470 (1989).  
<sup>8</sup>V. H. Grassian, E. R. Bernstein, H. V. Secor, and J. I. Seeman, *J. Phys. Chem.* **94**, 6691 (1990).  
<sup>9</sup>W. Drescher, S. Kendler, S. Zilberg, E. Zingher, H. Zuckermann, and Y. Haas, *J. Chem. Phys.* **101**, 11082 (1994).  
<sup>10</sup>W. E. Sinclair, H. Yu, D. Philips, R. D. Gordon, J. M. Hollas, S. Klee, and G. Mellau, *J. Phys. Chem.* **99**, 4386 (1995).  
<sup>11</sup>M. H. Hui and S. A. Rice, *J. Chem. Phys.* **61**, 833 (1974).  
<sup>12</sup>J. A. Syage, F. Al Adel, and A. H. Zewail, *Chem. Phys. Lett.* **103**, 15 (1983).  
<sup>13</sup>C. M. Harper and J. M. Hollas, *Chem. Phys. Lett.* **226**, 577 (1994).  
<sup>14</sup>J. P. Finley and J. R. Cable, *J. Phys. Chem.* **97**, 4595 (1993).  
<sup>15</sup>J. R. Cable and N. R. Westrick, *J. Chem. Phys.* **101**, 6455 (1994).  
<sup>16</sup>The original estimate of the equilibrium torsional angle from Ref. 15 of  $23^\circ$  was based in part on semiempirical AM1 calculations which have recently been repeated at the *ab initio* 3-21G level to yield the  $45^\circ$  value. These calculations also result in two equivalent ground state conformations which do not interconvert over a low energy barrier along an adiabatic torsional coordinate.  
<sup>17</sup>L. H. Scharpen and V. W. Laurie, *J. Chem. Phys.* **49**, 3041 (1968).  
<sup>18</sup>T. Stroyer-Hansen and E. Norby-Svendsen, *Spectrochim. Acta* **36A**, 359 (1980).  
<sup>19</sup>W. C. Wiley and I. H. McLaren, *Rev. Sci. Instrum.* **26**, 1150 (1955).  
<sup>20</sup>W. F. Bailey and T. V. Ovaska, *Tetrahedron Lett.* **31**, 627 (1990).  
<sup>21</sup>D. R. Arnold and S. A. Mines, *Can. J. Chem.* **67**, 689 (1989).  
<sup>22</sup>W. J. Buma, B. E. Kohler, J. M. Nuss, T. A. Shaler, and K. Song, *J. Chem. Phys.* **96**, 4860 (1992).  
<sup>23</sup>D. G. Lister, J. N. MacDonald, and N. L. Owen, in *Internal Rotation and Inversion* (Academic, New York, 1978), Chap. 2.  
<sup>24</sup>K. S. Pitzer, *J. Chem. Phys.* **14**, 239 (1946).  
<sup>25</sup>J. J. P. Stewart, MOPAC ver. 5.00. Quantum Chemistry Program Exchange No. 455, Department of Chemistry, Indiana University, Bloomington, IN.  
<sup>26</sup>J. D. Lewis, T. B. Malloy, Jr., T. H. Chao, and J. Laane, *J. Mol. Struct.* **12**, 427 (1972).  
<sup>27</sup>J. B. Coon, N. W. Naugle, and R. D. McKenzies, *J. Mol. Spectrosc.* **20**, 107 (1966).  
<sup>28</sup>C. Manneback, *Physica* **17**, 1001 (1951).  
<sup>29</sup>SPARTAN ver. 3.0 Wavefunction, Inc., Irvine, CA.  
<sup>30</sup>T. R. Rizzo, Y. D. Park, L. A. Peteanu, and D. H. Levy, *J. Chem. Phys.* **84**, 2534 (1986); Y. D. Park, T. R. Rizzo, L. A. Peteanu, and D. H. Levy, *ibid.* **84**, 6539 (1986).  
<sup>31</sup>J. P. Finley and J. R. Cable, *J. Phys. Chem.* **98**, 3950 (1994).  
<sup>32</sup>Q. Shen, O. V. Dorofeeva, V. S. Mastryukov, and A. Almeninngen, *J. Mol. Struct.* **246**, 237 (1991).  
<sup>33</sup>E. B. Wilson, Jr., J. C. Decius, and P. C. Cross, in *Molecular Vibrations; the Theory of Infrared and Raman Vibrational Spectra* (McGraw-Hill, New York, 1955).  
<sup>34</sup>S. I. Chan, J. Zinn, and W. D. Gwinn, *J. Chem. Phys.* **34**, 1319 (1961).  
<sup>35</sup>T. B. Malloy, Jr. and W. J. Lafferty, *J. Mol. Spectrosc.* **54**, 20 (1975).  
<sup>36</sup>T. B. Malloy, Jr., *J. Mol. Spectrosc.* **44**, 504 (1972).  
<sup>37</sup>J. Laane, M. A. Harthcock, P. M. Killough, L. E. Bauman, and J. M. Cooke, *J. Mol. Spectrosc.* **91**, 286 (1982).